TU Delft

Delft University of Technology

Document Version
Final published version

Licence
Dutch Copyright Act (Article 25fa)

Citation (APA)
Ritmejeris, J., Chen, X., Albada, B., & Dekker, C. (2026). Terminal Conjugation Enables Nanopore Sequencing of Peptides. *Journal of the American Chemical Society*, *148*(3), 3433-3441. https://doi.org/10.1021/jacs.5c18813

Important note
To cite this publication, please use the final published version (if applicable).
Please check the document version above.

Copyright
In case the licence states “Dutch Copyright Act (Article 25fa)”, this publication was made available Green Open Access via the TU Delft Institutional Repository pursuant to Dutch Copyright Act (Article 25fa, the Taverne amendment). This provision does not affect copyright ownership.
Unless copyright is transferred by contract or statute, it remains with the copyright holder.

Sharing and reuse
Other than for strictly personal use, it is not permitted to download, forward or distribute the text or part of it, without the consent of the author(s) and/or copyright holder(s), unless the work is under an open content license such as Creative Commons.

Takedown policy
Please contact us and provide details if you believe this document breaches copyrights.
We will remove access to the work immediately and investigate your claim.

This work is downloaded from Delft University of Technology.

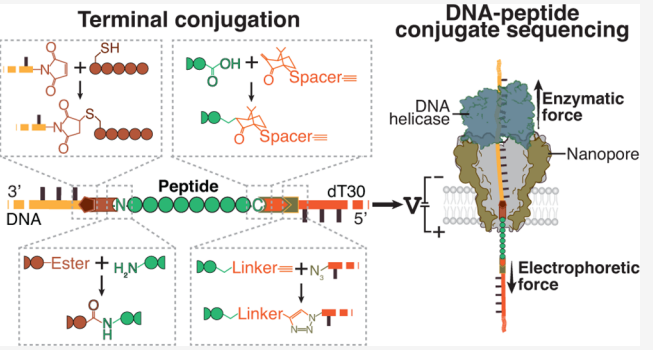
JACS
JOURNAL OF THE AMERICAN CHEMICAL SOCIETY
pubs.acs.org/JACS
Article

Terminal Conjugation Enables Nanopore Sequencing of Peptides

Justas Ritmejeris, Xiuqi Chen, Bauke Albada, and Cees Dekker*

Cite This: J. Am. Chem. Soc. 2026, 148, 3433−3441
Read Online
ACCESS | Metrics & More | Article Recommendations | Supporting Information

ABSTRACT: Nanopore sequencing of peptides holds great promise for single-molecule proteomics, but robust conjugation strategies to adapt native peptides for motor-enzyme−driven translocation have yet to be developed. Here, we establish terminally directed DNA−peptide conjugation chemistry strategies that expand the applicability of nanopore sequencing beyond synthetic model systems to natural peptides. At the N terminus, omniligase catalyzes rapid and peptide ligation of a DNA handle under mild conditions. At the C terminus, photoredox decarboxylative ligation introduces a bioorthogonal linker that enables CuAAC-mediated DNA attachment that ensures proper stretching and translocation of short peptides through the nanopore. Our study reveals that long peptides can be sequenced with single-end conjugation, while short or neutral peptides require threading tails. Positively charged peptides cannot be translocated under the same electric field but can be sequenced after charge neutralization. The data demonstrate controlled nanopore readouts of peptides that differ widely in length, charge, and sequence. This framework establishes a versatile chemical foundation for adapting natural peptides to nanopore sequencing, advancing single-molecule proteomic analysis.



Downloaded via TU DELFT on March 13, 2026 at 15:48:15 (UTC).
See https://pubs.acs.org/sharingguidelines for options on how to legitimately share published articles.

INTRODUCTION

Nanopore sequencing has transformed genomics and transcriptomics by providing single-molecule analysis of DNA and RNA.[1−3] Extending this capability to peptides and proteins would enable direct observation of proteoforms, post-translational modifications, and molecular heterogeneity − all at a single-molecule level inaccessible to mass spectrometry.[4,5] However, protein sequencing faces various significant challenges. For example, peptides lack the uniform negative charge and predictable structure of nucleic acids, preventing reliable electrophoretic capture and controlled translocation through nanopores. Furthermore, free translocation of proteins yields very short residence times in the nanopore,[6] which prevents their accurate analysis. Motor enzymes have proven essential for achieving nanopore sequencing by enforcing directional movement and slowing analyte translocation to the (sub)second time scales.[7,8] The protein unfoldase ClpX for example was shown to induce translocation of full-length proteins.[9−11] However, ClpX requires specific recognition tag for substrate engagement and often displays irregular multi-residue step sizes,[12] which limits its general applicability for high-resolution sequencing.

DNA−peptide conjugation has emerged as an alternative strategy that incorporates the exceptional processivity and precision of DNA motor enzymes to control analyte movement through nanopores.[13−15] By attaching DNA handles to peptides, molecular motor proteins like DNA helicases can control peptide translocation while maintaining their native stepping behavior on the DNA strand (Figure 1A). For example, the helicase Hel308 provide a uniform ∼0.3 nm step size along DNA with minimal backtracking, enabling 2 steps per base resolution in nanopore DNA sequencing platforms.[16] Proof-of-concept studies demonstrated single−amino acid resolution in peptide translocation[13] as well as PTM detection[17,18] using this approach. Similarly, DNA-conjugate sequencing strategies have recently been applied to glycan analysis,[19] demonstrating broader applicability of this sequencing approach across different classes of biomolecules. However, these studies relied exclusively on synthetic biopolymers with preinstalled cysteines or bioorthogonal handles for conjugation to DNA, limiting its general applicability. Such requirements preclude the analysis of native molecules derived from biological samples, where modification sites cannot be predetermined.

Several chemical and enzymatic methods have been explored for terminal peptide modifications, but each of these is subject to specific sequence requirements or reaction conditions. At the N terminus of peptides, a wide variety of strategies are available.[20] Native chemical ligation and transamination-based

Received: October 24, 2025
Revised: December 29, 2025
Accepted: December 31, 2025
Published: January 9, 2026



© 2026 American Chemical Society

https://doi.org/10.1021/jacs.5c18813
J. Am. Chem. Soc. 2026, 148, 3433−3441

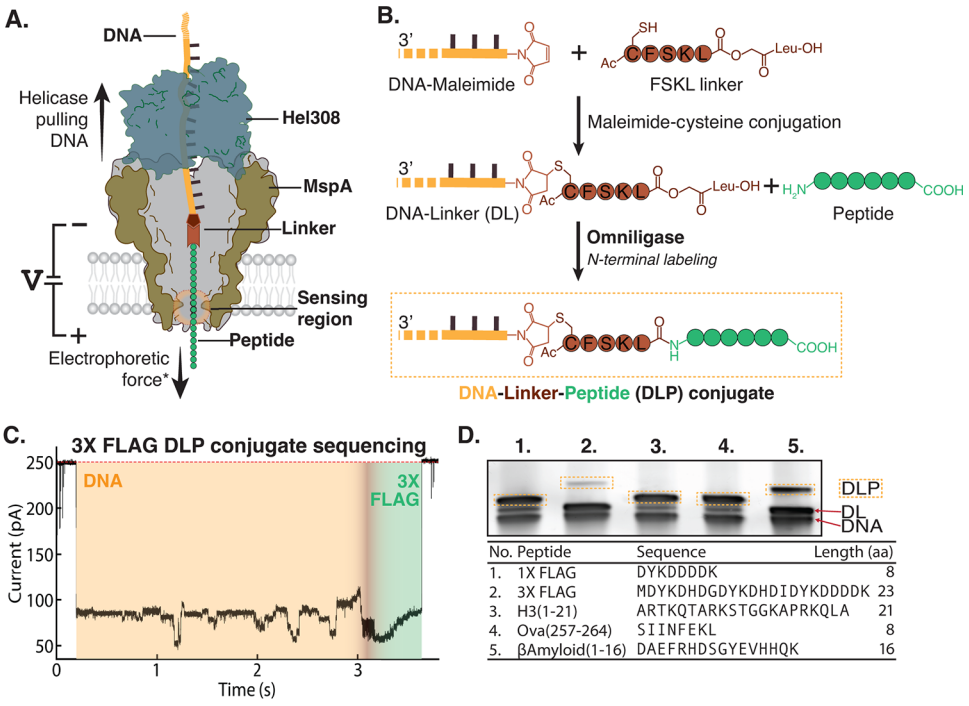


Figure 1. Omniligase enables site-specific N-terminal DNA conjugation of peptides compatible with nanopore sequencing. (A) Schematic depiction of nanopore sequencing of DLP constructs. Under an applied voltage (+180 mV), negatively charged DLP molecules are electrophoretically driven into MspA-M2(N93D) pores until stopped by the Hel308 motor enzyme, which subsequently pulls the DNA back through the pore. Corresponding ionic current changes can be assigned to the DNA, linker, and peptide segments as they traverse the sensing region. (B) Schematic depiction of the N-terminal conjugation strategy. First, a DNA oligonucleotide with a maleimide group is coupled to a cysteine-containing FSKL linker. The resulting DNA−linker (DL) conjugate is ligated to the peptide of interest using omniligase enzyme, yielding a DNA−linker−peptide (DLP) construct. (C) Representative nanopore trace of a urea-PAGE-purified 3X FLAG DLP construct recorded using MinION flowcells containing MspA-M2(N93D) pores, showing a DNA region followed by a gradual transition into the linker and then into the peptide segment. Sequencing was performed in cis buffer containing 500 mM KCl, 10 mM HEPES, 10 mM $MgCl_2$, and 1 mM ATP. (D) Urea-PAGE (10%) analysis of DLP formation with various peptides. Distinct band shifts confirmed peptide attachment to the DL with varying ligation efficiencies.

methods are highly specific in controlled contexts but their applicability is restricted by sequence dependence, i.e. it requires specific amino acids at the N terminus.[21−23] *N*-hydroxysuccinimide (NHS)-esters are widely used but typically modify not merely the N-terminal but also all lysine side chains.[24] 2-pyridinecarboxaldehyde (2-PCA) reagents provide a versatile approach that disfavors only proline in the second residue, but it requires extended reaction times and a high excess of reagents.[25−28] At the C terminus, enzymatic strategies using Sortase A enable efficient ligation but this approach relies on the engineered LPXTG motif, limiting its generalization.[29,30] More broadly, bifunctional cross-linking chemistries can connect DNA to peptides but often yield heterogeneous mixtures.[31,32] Despite progress in protein labeling strategies, no existing method provides a universal, and terminal-specific strategy for DNA attachment at both termini of natural peptides.

Here we developed terminal conjugation strategies of adapting native peptides for nanopore sequencing. We integrate enzymatic N-terminal ligation with chemical C-terminal functionalization to create DNA−peptide−DNA conjugates. Enzymatic N-terminal ligation was achieved with omniligase, which can couple peptides to a DNA-linker intermediate within minutes under mild conditions.[33] Although broadly sequence-tolerant, this reaction is influenced by the two residues at the N-terminal of the target peptide,[34] and hence we developed a strategy to avoid this dependence. At the C terminus, photoredox-mediated decarboxylation was used to selectively activate the terminal carboxylate, enabling installation of an alkyne-containing linker under visible-light irradiation.[35,36] Subsequent copper-catalyzed azide−alkyne cycloaddition (CuAAC) coupling[37] of an azide-functionalized DNA tail provided constructs with enhanced capture and stretching properties. Together, these chemistries offer orthogonal and broad-sequence compatibility to both termini of natural peptides.

By combining these chemical strategies, we analyze diverse peptides ranging in length from 8−26 residues with highly varying charge profiles. We establish key design rules for nanopore sequencing approaches. Specifically, (i) longer peptides (>∼20 amino acids) with a net negative charge can be analyzed using N-terminal conjugation alone, (ii) shorter peptides require an additional C-terminal DNA for stable capture and translocation, and (iii) chemical neutralization of positively charged peptides enables sequencing of cationic peptides that are otherwise excluded by electrostatic repulsion. These terminal-conjugation strategies provide the first general method for adapting native peptides to motor-driven nanopore sequencing, establishing a chemical foundation for single-molecule proteomic applications.

https://doi.org/10.1021/jacs.5c18813
J. Am. Chem. Soc. 2026, 148, 3433−3441

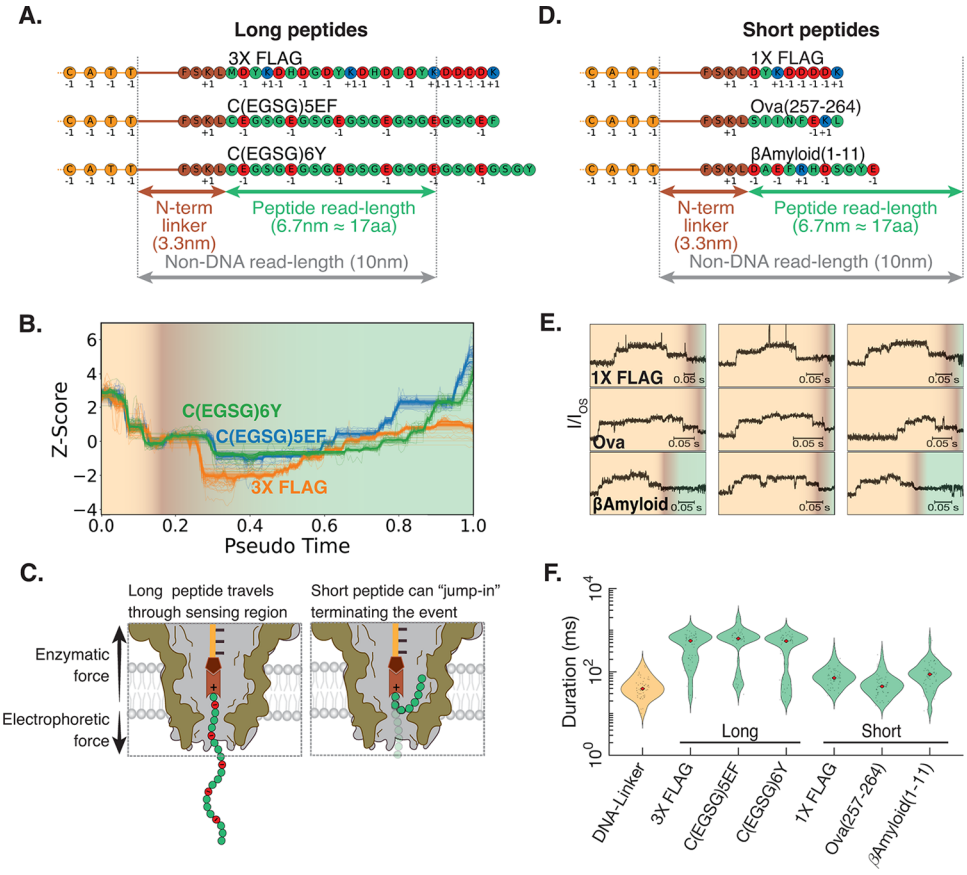


Figure 2. Nanopore sequencing of DLP conjugates reveals robust readout for long peptides but inconsistent signals for short peptides. (A) Schematic of DLP constructs containing long peptides of interest (23−26 amino acids) that are to be read in nanopore sequencing. The conjugates consist of DNA (orange), an FSKL linker (brown), and peptides with neutral (green), with negatively (red) or positively (blue) charged residues. Nanopore read length is primarily determined by the distance between the Hel308 docking site and the sensing region (10 nm for MspA). (B) Dynamic time warping (DTW) alignment of peptide-region signals for long-peptide DLP constructs: 3X FLAG (orange, N = 110), C(EGSG)$_5$EF (blue, N = 97), and C(EGSG)$_6$Y (green, N = 63). Gradient colors indicate transition from DNA (light yellow) to linker (brown) and peptide (green) regions. (C) Schematic depiction of a DNA motor enzyme pulling a negatively charged DLP conjugate through MspA. Electrophoretic force drives the construct into the pore, while the stronger enzymatic force ratchets it upward, resulting in a stretched conjugate that traverses the sensing region in a controlled fashion, while the bottom section behaves as an anchor to prevent premature event termination (left); for short-peptide sequencing, the positively charged linker and heterogeneous peptide sequence can enter the nanopore vestibule during the sequencing event, prematurely terminating events and generating inconsistent signals at the peptide segment (right). (D) Schematic of DLP constructs containing short peptides of interest (8−11 amino acids). (E) Representative nanopore sequencing time traces of short-peptide DLP constructs showing the transition from DNA (light yellow) to linker (light brown) to peptide (light green) regions. Scale bars represent individual event durations in seconds. Ion currents (I) are normalized to the local unblocked open-state pore current (I_{OS}). All plots display the 0.3 − 0.65 I/I_{OS} range. (F) Duration of the peptide segment in the nanopore constriction for different urea-PAGE-purified DLP constructs. DNA−linker (yellow) serves as a control to identify events lacking a peptide signal (median = 43 ms). Long-peptide constructs (3X FLAG, C(EGSG)$_5$EF, and C(EGSG)$_6$Y) show extended peptide-region dwell times (medians: 575, 635, and 562 ms, respectively). Short-peptide constructs (1X FLAG, Ova(257−264), and βAmyloid(1−11)) show markedly shorter durations (72, 44, and 89 ms, respectively). n = 65 events per construct were used for analysis.

RESULTS

Omniligase Enables Rapid N-Terminal DNA Conjugation across Diverse Peptide Sequences

To systematically evaluate peptide conjugation and sequencing performance, we assembled a panel of 11 peptides spanning 8−26 residues (Supplementary Table 1). This captures a representative range of peptides of various length, charge, and sequence contexts encountered in natural samples.

To enable DNA motor-driven nanopore sequencing of natural peptides, a DNA handle was introduced at the N-terminus of the peptide. Omniligase catalyzes scarless peptide bond formation between an N-terminal amino group of a substrate peptide and a small acyl donor peptide carrying a C-terminal − OCam-LeuOH activating ester.[34] To adapt this chemistry for DNA−peptide conjugation, we synthesized a DNA oligonucleotide bearing a 5′-maleimide group and coupled it to a pentapeptide Ac-CFSKL-OCam-LeuOH (linker peptide) via maleimide−cysteine chemistry (Figure 1B and Supplementary Figure 1). The resulting DNA−linker (DL) (Supplementary Figure 2) served as the acyl donor for omniligase-mediated ligation with peptides of interest, yielding DNA−linker−peptide (DLP) conjugates (Figure 1B, bottom). Such DLPs can then be subject to sequencing with the MspA nanopore/Hel308 helicase system. Once the DLP is bound by the Hel308 in bulk, it is electrophoretically driven into the pore and halted as the helicase is drawn on top of the MspA nanopore (Figure 1A). The partial blockade of the nanopore

https://doi.org/10.1021/jacs.5c18813
J. Am. Chem. Soc. 2026, 148, 3433−3441

constriction region (i.e., its narrowest part) produces step-like ionic current signatures as the helicase pulls the molecule upward against the electric field (Figure 1C). The peptide signals immediately follow the well-characterized DNA signals, allowing for sensitive characterizing of the peptide properties.[13]

We performed omniligase-ligation-based preparation of DLPs and evaluated the ligation efficiency by urea PAGE. Distinct band shifts confirmed successful conjugation (Figure 1D, Supplementary Figure 3). As the reaction reached maximal yield within 5 min at room temperature (see H3(1−21) peptide data in Supplementary Figure 4), this method appears to be compatible with time- or temperature-sensitive samples.[38] Conjugation yields depended on peptide sequence and varied from 23% for the 3X FLAG peptide to 67% for the H3(1−21) peptide, with averages determined from three independent reactions. Consistent with prior reports, efficiency depended on the N-terminal residues of the acceptor peptide.[34,39,40] Additional factors such as charge profile, length, and peptide solubility however also influence ligation efficiency. To validate that the shifted bands corresponded to ligated peptides, 1X and 3X FLAG DLPs were isolated by affinity purification using anti-FLAG resin, yielding a clear conjugate band at the same location (Supplementary Figure 5). All DLP conjugates were purified by cutting the bands from the acrylamide gel before nanopore sequencing. An example is given in Figure 1C, which shows that the 3X FLAG peptide produced a distinct signal pattern after the DNA. At the boundary between DNA and peptide, we observed a period of rapid signal fluctuation, which likely relates to the movement of the opposing charges on the peptide (positively charged lysine and negatively charged aspartate) across the pore. Further into the peptide segment, the signals exhibited a reproducible signature with a slightly rising feature before returning to open pore level, when the DLP was ejected from the nanopore. With wide compatibility of peptide sequences for the omniligase,[34] this workflow creates a facile conjugation reaction for labeling N-terminus of various peptides.

Single-Terminal Conjugation Allows for Robust Measurement of Long Peptides but not Short Ones

Next, we examined the range of peptide lengths possible for omniligase-facilitated nanopore sequencing. Encouragingly, a large fraction of long peptide sequencing events (23−26 residues, Figure 2A) showed reproducible ionic current patterns with each variant displaying a characteristic signal profile that enabled discrimination (Figure 2B, Supplementary Figure 6). The maximal peptide read length in MspA corresponds to the distance between the helicase docking site and the sensing region, which is about 10 nm.[13,41] For DLPs, this distance covers the FSKL-linker (3.3 nm) and the first ∼17 amino acids (6.7 nm) if the molecule would adopt a linear stretched configuration. Accordingly, $C(EGSG)_5EF$ and $C(EGSG)_6Y$, which share the first 22 residues, produced nearly identical signals, but diverge in the later sections of the trace (Figure 2B). This divergence reflects the influence of the differing C-terminal regions (F vs GSGY). Note that the peptide does not adopt a straightened conformation due to insufficient stretching with low density of negative charge (Figure 2C, left), and hence the influence of the residues can be more distant than for a fully stretched linear peptide.[13,42] As a result, residues beyond the ∼17 amino acid sensing window can still influence the ionic current through conformational effects and interactions with the pore. These results demonstrate that long peptides produce reproducible, discriminative signatures that enable variant identification even with closely resembling sequences.

By contrast, short peptides (8−11 residues) (Figure 2D) were harder to detect and did not yield reproducible ionic current patterns, with individual events showing inconsistent signals (Figure 2E, Supplementary Figure 7). Although their length could in principle lead to a full translocation through the sensing region before helicase disengagement, most peptide variants displayed only very short signals, reducing a likelihood of precise peptide identification. Instead of consistent, stepwise signal traces, short peptide constructs frequently terminated prematurely and rarely demonstrated robust peptide signatures after the DNA trace, suggesting an unstable movement of the peptide across the nanopore constriction. We attribute this variability to the short length of the peptide within the pore (Figure 2C, right), which causes instability during translocation, and makes the peptide sensitive to thermal fluctuations as well as to interactions with the nanopore surface. This effect may be further amplified by a positively charged lysine residue in the linker, which reduces the effective electrophoretic stretching force acting on the peptide. In this regime, the electrophoretic force is insufficient to maintain tension across the molecule. This instability is also reflected in the peptide-region signal durations (Figure 2F), which showed markedly shorter dwell times (44−89 ms) for short-peptide constructs − closely matching the dwell time of DNA-linker events (43 ms) − in contrast to the longer peptides (562−635 ms). These results indicate that short peptides occupy the sensing region only briefly before escaping the nanopore.

To exclude purification artifacts as the source of variability, we compared urea-PAGE-purified samples (which often showed less pronounced DLP separation from DL for shorter peptides) with affinity-purified 1X and 3X FLAG DLPs obtained using anti-FLAG resin (Supplementary Figure 5). In both cases 1X FLAG peptide generated short signals while 3X FLAG peptide produced reproducible longer events with shorter events occurring only occasionally (Supplementary Figures 6−8). To confirm that short peptides were successfully conjugated as expected, we performed LC−MS analysis on PAGE-purified DLP samples of 1X FLAG and Ovalbumin (257−264), which confirmed the presence of complete DLP conjugates with predicted molecular masses (Supplementary Figures 9 and 10).

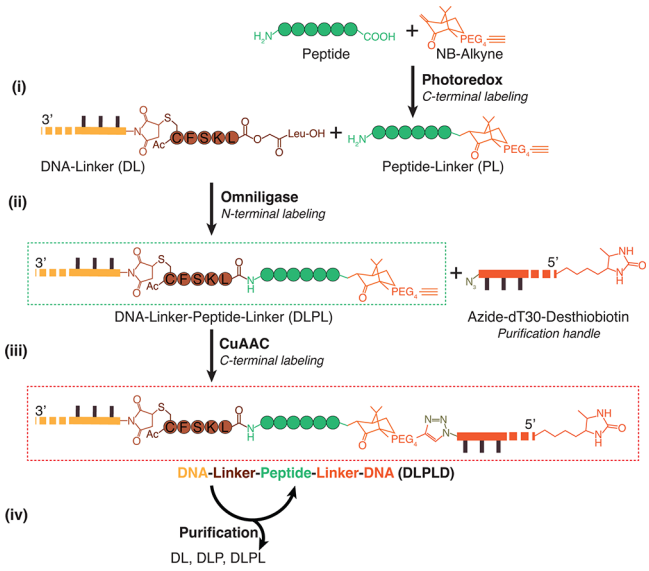
These findings suggest that single-end conjugation requires a long peptide with net negative charge for consistency in nanopore readings. Shorter peptides fail to translocate orderly within the pore and yield events that often contain only the DNA segment, while the peptide portion is generally absent or indistinct (Supplementary Figure 7). This motivated the attachment of C-terminal threading tails, which should stabilize short peptides in the nanopore and extend the range of sequences compatible with nanopore sequencing, as discussed next.

Conjugation at Both Peptide Termini Allows Nanopore Sequencing of a Broader Range of Peptides

To extend the applicability of DNA−peptide conjugates to short peptides, we developed a C-terminal modification strategy that installs a negatively charged threading tail, yielding DNA-linker-peptide-linker-DNA (DLPLD) conjugates (Scheme 1). In this approach, photoredox-mediated

https://doi.org/10.1021/jacs.5c18813
J. Am. Chem. Soc. 2026, 148, 3433−3441

Scheme 1. Combined N- and C-Terminal Conjugation Strategy for Constructing DNA−Peptide−DNA Conjugates[a]



[a](i) Photoredox-mediated decarboxylative C-terminal modification installs an NB−alkyne linker on the peptide of interest to yield a peptide−linker (PL) intermediate. (ii) N-terminal attachment of a DNA−linker (DL) via omniligase ligation affords a DNA−linker−peptide−linker (DLPL) construct. (iii) In the last step, the C-terminal alkyne is coupled to an azide-functionalized dT_{30} threading tail by CuAAC, producing the final DNA−linker−peptide−linker−DNA (DLPLD) conjugate. (iv) The dT_{30} threading tail with a desthiobiotin purification handle enables affinity purification with streptavidin-coated magnetic beads, thereby enriching DLPLD conjugates from unreacted intermediates.

single electron oxidation selectively activates the C-terminal carboxylate under visible-light irradiation with a lumiflavin photocatalyst. The short-lived carboxyl radical releases CO_2 to generate an α-amino alkyl radical, which then reacts to the Michael acceptor of the NB-alkyne linker, thereby installing a bioorthogonal alkyne handle at the peptide terminus.[35,36] Omniligase ligation, as previously described, can be directly implemented after photoredox modification of the peptide resulting in a DNA-linker-peptide-linker intermediate. This construct can be directly used for a CuAAC reaction to couple azide-dT_{30}-desthiobiotin construct as a threading tail using $CuSO_4$/THPTA complex with sodium ascorbate under mild reaction conditions.[37] The final DLPLD conjugate can be effectively purified and enriched using streptavidin-coated magnetic beads, which selectively capture the desthiobiotin-labeled products while removing unreacted DNA strands that could hinder nanopore sequencing. This workflow proceeds in aqueous conditions and is broadly compatible across very different peptide sequences.

As a proof of concept, we first applied this strategy to peptides that were validated using single-terminal conjugation. Formation of DLPLD conjugates was verified by urea-PAGE, which showed distinct bands corresponding to each intermediate and the final product (Figure 3A). With each added molecular component, the conjugate molecule showed lower electro-mobility during urea-PAGE (Figure 3A). After the full conjugation workflow, peptides carried a segment of DNA on both the N-terminus and C-terminus and showed a distinct band of the full conjugate (DLPLD).

We then proceeded to sequence the DLPLD constructs of short peptides with nanopores (Figure 3B). With a negatively charged DNA segment as the threading tail, the short peptides − which earlier failed in the DLP sequencing approach −

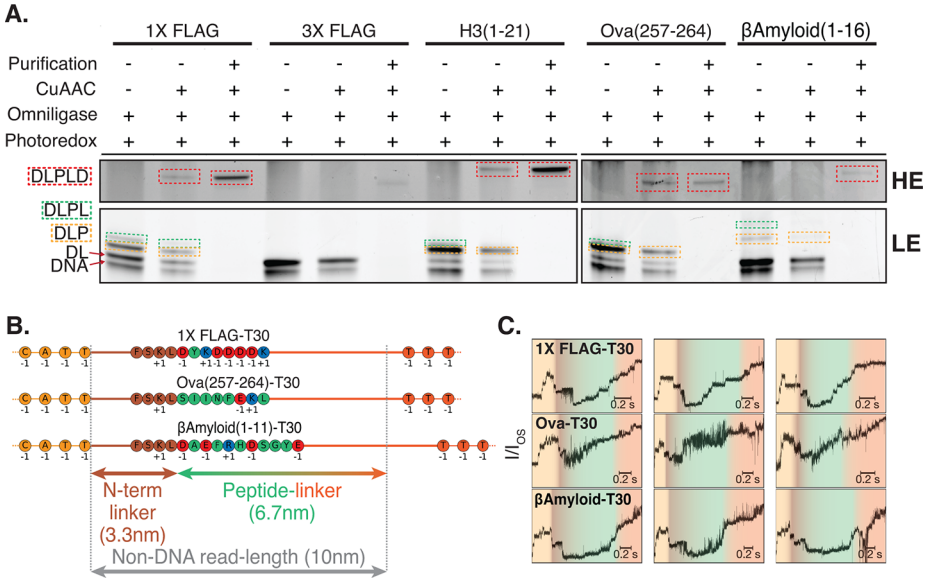


Figure 3. C-terminal conjugation enables threading tail attachment that is essential for sequencing short peptides. (A) Urea-PAGE (10%) analysis of DLPLD formation with various peptides. Distinct band shifts confirmed successive conjugation steps, high-exposure (HE) and low-exposure (LE) regions. Each peptide was analyzed in intermediate steps: after photoredox and omniligase ligation (Lane 1), after CuAAC reaction (Lane 2), and after affinity purification with streptavidin (Lane 3). Rectangles highlight reaction products: DLP (yellow), DLPL (green), and DLPLD (red). (B) Linear schematic of DLPLD constructs of varying length. Depending on peptide length and charge profile, a fraction of the threading tail (orange) can enter the MspA before the sequencing event ends. (C) Representative nanopore time traces of short-peptide DLPLD constructs with a threading tail. Gradient colors indicate transitions from DNA (light yellow) to linker (brown), peptide (green), and threading tail (orange) regions. Ion currents (I) are normalized to the local unblocked open-state pore current (I_{OS}). All plots are shown in the 0.3 − 0.65 I/I_{OS} range.

https://doi.org/10.1021/jacs.5c18813
J. Am. Chem. Soc. 2026, 148, 3433−3441

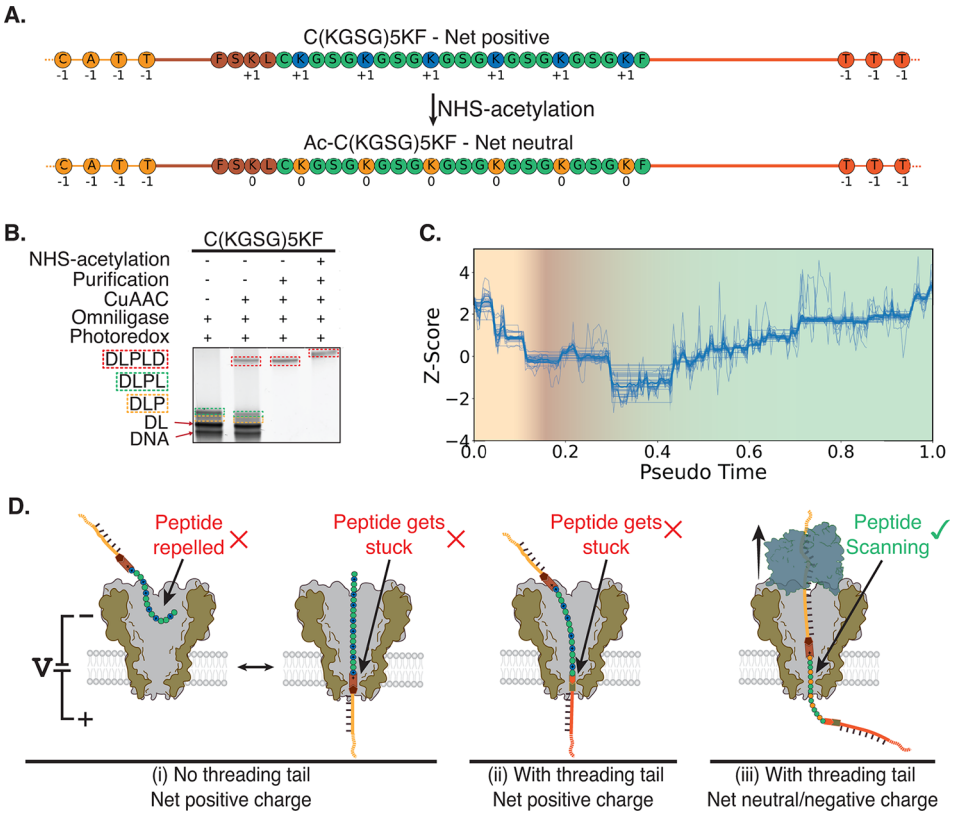


Figure 4. Chemical charge neutralization enables nanopore sequencing of positively charged peptides. (A) Linear schematic of $C(KGSG)_5KF$ peptide before and after neutralization by NHS ester acetylation of lysine side chains. (B) Urea-PAGE (10%) analysis of DLPLD formation of $C(KGSG)_5KF$ peptide. Peptide was analyzed in intermediate steps: after photoredox and omniligase ligation (Lane 1), after CuAAC reaction (Lane 2), after affinity purification with streptavidin (Lane 3), and after NHS-acetylation (Lane 4). Rectangles indicate reaction products: DLP (yellow), DLPL (green), and DLPLD (red). (C) Dynamic time warping (DTW) alignment of peptide-region timetraces for the Ac−$C(KGSG)_5KF$ DLPLD construct (N = 38). Gradient colors indicate transition from DNA (light yellow) to linker (brown) and peptide (green) regions. (D) Schematic models of charge-dependent translocation scenarios. (i) Peptide lacking a threading tail and carrying a net positive charge is unlikely to enter the pore peptide-first and may instead engage in bidirectional "tug-of-war" when entering DNA-first. (ii) Positively charged peptide with a threading tail could enter the pore, but the positively charged region may fail translocating to the bottom side due to bidirectional electrophoretic forces affecting the molecule. (iii) Neutral or negatively charged peptide with a threading tail can translocate through the nanopore more efficiently, allowing Hel308-mediated nanopore sequencing.

acquired better stretching during translocation, allowing prolonged measurements (Figure 3C). Representative nanopore traces of short-peptide DLPLD constructs revealed distinct signals of the peptides that varied for different sequences. Both 1X FLAG and βAmyloid(1−11) constructs generated reproducible signatures under these conditions. These findings indicate that C-terminal threading tails enables capture and stable readout of short peptides.

However, Ova(257−264), with a net neutral charge profile, generated more variable signals. This behavior is consistent with a weaker electrophoretic stretching inside the pore, which likely permits greater conformational freedom of the peptide backbone, yielding broader current distributions, a phenomenon also observed in a recent study.[43] While weaker stretching can thus introduce variability, a previous study reported sequence-specific differences that remained discernible with a very high precision,[17] indicating that sequencing can likely still resolve peptide variants even under reduced electrophoretic tension when a threading tail is installed in the DLPLD.

We observed that most peptides tolerated photoredox modification without any loss of ligation efficiency in the subsequent omniligase reaction (Supplementary Figure 11). Thus, omniligase remained active in the presence of photoredox reaction components, allowing the two steps to be performed sequentially without intermediate purification. While this strategy was effective for most peptides (8/11, see Supplementary Table 3), some peptides showed reduced yields after photoredox-mediated ligation. Control experiments indicated that the decrease arose from peptide-specific degradation in the presence of lumiflavin and 445 nm irradiation, rather than from enzyme inhibition (Supplementary Figure 12). A subset of peptides showed greater sensitivity to the degradation. In particular, the 3X FLAG peptide produced no detectable ligation product (Figure 3A), while $C(EGSG)_5EF$ and $C(QGSG)_5QF$ exhibited markedly reduced yields compared to reactions performed without photoredox treatment (Supplementary Figures 4 and 11).

Charge Neutralization Enables Nanopore Sequencing of Positively Charged Peptides

Positively charged peptides such as $C(KGSG)_5KF$ and H3(1−21) histone peptide conjugates remained among the most challenging substrates for nanopore sequencing. This is not surprising since they are subjected to an upward electrophoretic force on the cationic residues, which oppose the downward forces on DNA and negatively charged peptides.

https://doi.org/10.1021/jacs.5c18813
J. Am. Chem. Soc. 2026, 148, 3433−3441

Even when equipped with threading tails, we found that these peptides failed to translocate. To overcome this limitation, we used NHS ester to acetylate the lysine side chains of $C(KGSG)_5KF$ construct, thereby removing the net positive charge (Figure 4A). Formation of such chemically altered DLPLD conjugates was verified by urea-PAGE, which showed distinct gel bands corresponding to each reaction step. The clean band shift after NHS-mediated acetylation, with no detectable initial product, indicated highly efficient labeling of lysine residues (Figure 4B).

Attempts of nanopore sequencing of acetylated and nonacetylated constructs demonstrated the critical role of charge neutralization. After treating $C(KGSG)_5KF$ peptide with sulfo-NHS-acetate, the DLPLD of acetylated peptide ($Ac-C(KGSG)_5KF$) was successfully identified in nanopore sequencing. Dynamic time warping (DTW) signal alignment[44] revealed reproducible peptide-region signals for $Ac-C(KGSG)_5KF$ (Figure 4C), in contrast to absent signals observed for the nonacetylated variant. Notably, the acetylated construct displayed higher signal amplitude and increased noise within the peptide region, as similarly observed for the weakly charged Ova(257−264) DLPLD analyte, suggesting weaker electrophoretic stretching of the neutralized peptide during translocation. The findings confirm that reducing cationic charge restored the sequencing ability and provided distinct signals for previously positively charged peptide. These findings align with prior observations that opposing electrophoretic force can trap or repel opposing charge peptides.[45−47]

Figure 4D sketches the variety of charge-dependent threading of peptides through a nanopore. Positively charged peptides lacking threading tails are unable to enter peptide-first (Figure 4D(i), left). Instead, upon entering DNA-first, they typically engage in a bidirectional "tug-of-war" where the negatively charged DNA handle are subjected to a downward electrophoretic force while the positively charged peptide experiences an opposing upward force (Figure 4D(i), right).[47] When equipped with a negatively charged threading tail, such peptides can enter the pore but subsequently experience similar opposing electrophoretic forces (Figure 4D(ii)). The downward force on the DNA and threading tail competes with the upward force on the positively charged peptide region, preventing complete translocation and causing the molecule to become trapped within the nanopore. By contrast, tailed peptides with neutral or negative charge are expected to pass sensing region, which subsequently enables Hel308 to ratchet the analyte through the sensing region for sequencing (Figure 4D(iii)). Together, these results demonstrate that chemical charge neutralization provides a practical solution for expanding nanopore sequencing to highly basic peptides. More broadly, they establish charge modulation as a generalizable design principle for adapting diverse peptide substrates to nanopore analysis.

DISCUSSION AND CONCLUSIONS

This study establishes a set of design rules for adapting natural peptides to nanopore sequencing by developing terminal conjugation strategies and evaluating the effects of peptide length and charge on nanopore sequencing. Attachment of a DNA handle at one terminus provides a general entry point for DNA motor-driven peptide sequencing. Longer and negatively charged peptides yield reproducible and discriminative ionic current patterns, whereas short peptides require additional conjugation. DNA-peptide-DNA constructs enable sequencing of short and neutral peptides by enforcing capture through a negatively charged threading tail and promoting sufficient peptide stretching. Finally, chemical neutralization of positively charged peptides that would otherwise resist nanopore translocation enables sequencing of such analytes. These rules are based on representative examples from our peptide panel; systematic determination of quantitative relationships between charge density, peptide length, and translocation efficiency remains an important direction for future work. This study defines a versatile chemical toolset for adapting diverse peptides to nanopore sequencing.

The terminal conjugation chemistries introduced in this study combine enzymatic and chemical approaches to access both peptide termini under mild and orthogonal conditions. At the N terminus, omniligase provides rapid, sequence-tolerant peptide bond formation between a DNA-linked acyl donor and the target peptide, yielding DNA−peptide conjugates. At the C terminus, photoredox decarboxylation enables site-specific activation of the terminal carboxylate, installing an alkyne linker that can be coupled to azide-modified DNA through CuAAC.

While our work demonstrates feasibility across representative peptides, it offers several opportunities for further optimization. At the N terminus, the DNA-linker intermediate is based on a pentapeptide acyl donor (Ac-CFSKL-OCamLeu) containing a positively charged residue. Introducing negatively charged amino acids here in the linker may improve electrophoretic capture and yield more uniform translocation behavior of the analyte. However, because the last four C-terminal residues of the acyl donor critically influence ligation efficiency, such modifications must be carefully designed to avoid interfering with omniligase activity.[34,40] Structural and mechanistic analysis of omniligase activity reveals specific requirements for positions in the acyl donor sequence. Future design of the pentapeptide could incorporate negatively charged amino acid replacing serine, and the positively charged lysine could be replaced by neutrally charged amino acid. While omniligase-mediated conjugation provides broad sequence compatibility for N-terminal labeling, there are design trade-offs to consider. The pentapeptide linker occupies ∼3.3 nm of the ∼10 nm sensing region, reducing effective peptide read length. Alternatively, chemistries such as 2-pyridinecarboxaldehyde (2-PCA) labeling could supplement omniligase in cases of low ligation efficiency or where shorter linker length is necessary.[25,27] At the C terminus, the current linker connecting DNA with a peptide is relatively long (4.9 nm) and electrically neutral; shortening it and/or introducing negative charges may enhance electrophoretic pulling forces, resulting in more consistent signal profiles, particularly for short or weakly charged sequences. Finally, integration of controlled electro-osmotic flow from the nanopore surface may provide more uniform stretching forces inside the nanopore, minimizing sequence-dependent fluctuations and yielding more reproducible readouts across various peptide substrates.[48−50]

Compared to prior nanopore peptide sequencing approaches, which relied on synthetic peptides with pre-engineered handles, our strategy broadens the accessible sample space to unmodified peptides. The sequence tolerance of our conjugation chemistries − which do not require preinstalled reactive groups or specific recognition motifs − enables analysis of native peptides or samples after protease digestion. This represents a critical step toward applying

https://doi.org/10.1021/jacs.5c18813
J. Am. Chem. Soc. 2026, 148, 3433−3441

nanopore sequencing to real proteomic samples, where peptide sequences cannot be preset. This work provides a chemical foundation for single-molecule proteomic analysis beyond synthetic model systems. Future integration with protease digestion workflows will further advance nanopore sequencing toward comprehensive, single-molecule proteome characterization.

■ ASSOCIATED CONTENT

Data Availability Statement

The processed data, processing scripts, analysis scripts, and plotting scripts for reproducing the figures are deposited in Zenodo (doi: 10.5281/zenodo.17949706).

Supporting Information

The Supporting Information is available free of charge at https://pubs.acs.org/doi/10.1021/jacs.5c18813.

Additional experimental details, materials, and methods, raw gel images, sequencing events, LC−MS analysis, and ^{1}H NMR spectra for NB-PEG$_4$-alkyne linker (PDF)

■ AUTHOR INFORMATION

Corresponding Author

Cees Dekker − *Department of Bionanoscience, Kavli Institute of Nanoscience Delft, Delft University of Technology, 2629 HZ Delft, The Netherlands;* orcid.org/0000-0001-6273-071X; Email: c.dekker@tudelft.nl

Authors

Justas Ritmejeris − *Department of Bionanoscience, Kavli Institute of Nanoscience Delft, Delft University of Technology, 2629 HZ Delft, The Netherlands;* orcid.org/0000-0002-6166-4594

Xiuqi Chen − *Department of Bionanoscience, Kavli Institute of Nanoscience Delft, Delft University of Technology, 2629 HZ Delft, The Netherlands;* orcid.org/0000-0003-1157-3501

Bauke Albada − *Laboratory of Organic Chemistry, Wageningen University & Research, 6807 WE Wageningen, The Netherlands;* orcid.org/0000-0003-3659-2434

Complete contact information is available at: https://pubs.acs.org/10.1021/jacs.5c18813

Funding

The research was partly funded by Oxford Nanopore Technologies (C.D.); This publication is cosupported by a grant from the National Growth Fund program Biotech Booster; X.C. acknowledges funding from the Dutch Research Council (NWO) under the Veni program with the grant ID VI.Veni.242.128. C.D. acknowledges funding from Dutch Research Council (NWO) grant NWO-I680, NWO-XL grant OCENW.XL21.XL21.003 (ProPore).

Notes

The authors declare no competing financial interest.

■ ACKNOWLEDGMENTS

The authors thank R. Eelkema, P. Bohlander, and J. Swaminathan for helpful discussions and technical assistance with the photoredox reaction; A. Koijen, S. van den Beelen, and L. van den Bos for valuable input on implementing the Omniligase reaction; J. Smith, M. Jordan, K. Sabharwal, and J. Wallace for discussions and for providing MinION flowcells; M. Peters for the LC−MS analysis of the DLP conjugates; J. Firet for peptide synthesis; and I. Nova, M. Filius, J. van der Sande, E. van der Sluis, J. van der Torre, L. Yu, T. Eriksson, T. Hoekstra, and B. Analikwu for helpful discussions.

■ REFERENCES

(1) Deamer, D.; Akeson, M.; Branton, D. Three Decades of Nanopore Sequencing. *Nat. Biotechnol.* **2016**, *34* (5), 518−524.

(2) Mohammadi, M. M.; Bavi, O. DNA Sequencing: An Overview of Solid-State and Biological Nanopore-Based Methods. *Biophys. Rev.* **2022**, *14* (1), 99−110.

(3) Dorey, A.; Howorka, S. Nanopore DNA Sequencing Technologies and Their Applications towards Single-Molecule Proteomics. *Nat. Chem.* **2024**, *16* (3), 314−334.

(4) Alfaro, J. A.; Bohländer, P. R.; Dai, M.; Filius, M.; Howard, C. J.; van Kooten, X. F.; Ohayon, S.; Pomorski, A.; Schmid, S.; Aksimentiev, A.; Anslyn, E. V.; Bedran, G.; Cao, C.; Chinappi, M.; Coyaud, E.; Dekker, C.; Dittmar, G.; Drachman, N.; Eelkema, R.; Goodlett, D. R.; Hentz, S.; Kalathiya, U.; Kelleher, N. L.; Kelly, R. T.; Kelman, Z.; Kim, S. H.; Kuster, B.; Rodriguez-Larrea, D.; Lindsay, S.; Maglia, G.; Marcotte, E. M.; Marino, J. P.; Masselon, C.; Mayer, M.; Samaras, P.; Sarthak, K.; Sepiashvili, L.; Stein, D.; Wanunu, M.; Wilhelm, M.; Yin, P.; Meller, A.; Joo, C. The Emerging Landscape of Single-Molecule Protein Sequencing Technologies. *Nat. Methods* **2021**, *18* (6), 604−617.

(5) MacCoss, M. J.; Alfaro, J. A.; Faivre, D. A.; Wu, C. C.; Wanunu, M.; Slavov, N. Sampling the Proteome by Emerging Single-Molecule and Mass Spectrometry Methods. *Nat. Methods* **2023**, *20* (3), 339−346.

(6) Plesa, C.; Kowalczyk, S. W.; Zinsmeester, R.; Grosberg, A. Y.; Rabin, Y.; Dekker, C. Fast Translocation of Proteins through Solid State Nanopores. *Nano Lett.* **2013**, *13* (2), 658−663.

(7) Manrao, E. A.; Derrington, I. M.; Laszlo, A. H.; Langford, K. W.; Hopper, M. K.; Gillgren, N.; Pavlenok, M.; Niederweis, M.; Gundlach, J. H. Reading DNA at Single-Nucleotide Resolution with a Mutant MspA Nanopore and Phi29 DNA Polymerase. *Nat. Biotechnol.* **2012**, *30* (4), 349−353.

(8) Cherf, G. M.; Lieberman, K. R.; Rashid, H.; Lam, C. E.; Karplus, K.; Akeson, M. Automated Forward and Reverse Ratcheting of DNA in a Nanopore at 5-Å Precision. *Nat. Biotechnol.* **2012**, *30* (4), 344−348.

(9) Nivala, J.; Marks, D. B.; Akeson, M. Unfoldase-Mediated Protein Translocation through an α-Hemolysin Nanopore. *Nat. Biotechnol.* **2013**, *31* (3), 247−250.

(10) Nivala, J.; Mulroney, L.; Li, G.; Schreiber, J.; Akeson, M. Discrimination among Protein Variants Using an Unfoldase-Coupled Nanopore. *ACS Nano* **2014**, *8* (12), 12365−12375.

(11) Motone, K.; Kontogiorgos-Heintz, D.; Wee, J.; Kurihara, K.; Yang, S.; Roote, G.; Fox, O. E.; Fang, Y.; Queen, M.; Tolhurst, M.; Cardozo, N.; Jain, M.; Nivala, J. Multi-Pass, Single-Molecule Nanopore Reading of Long Protein Strands. *Nature* **2024**, *633*, 662−669.

(12) Cordova, J. C.; Olivares, A. O.; Shin, Y.; Stinson, B. M.; Calmat, S.; Schmitz, K. R.; Aubin-Tam, M.-E.; Baker, T. A.; Lang, M. J.; Sauer, R. T. Stochastic but Highly Coordinated Protein Unfolding and Translocation by the ClpXP Proteolytic Machine. *Cell* **2014**, *158* (3), 647−658.

(13) Brinkerhoff, H.; Kang, A. S. W.; Liu, J.; Aksimentiev, A.; Dekker, C. Multiple Rereads of Single Proteins at Single-Amino Acid Resolution Using Nanopores. *Science* **2021**, *374*, 1509−1513.

(14) Chen, Z.; Wang, Z.; Xu, Y.; Zhang, X.; Tian, B.; Bai, J. Controlled Movement of ssDNA Conjugated Peptide through Mycobacterium Smegmatis Porin A (MspA) Nanopore by a Helicase Motor for Peptide Sequencing Application. *Chem. Sci.* **2021**, *12* (47), 15750−15756.

(15) Yan, S.; Zhang, J.; Wang, Y.; Guo, W.; Zhang, S.; Liu, Y.; Cao, J.; Wang, Y.; Wang, L.; Ma, F.; Zhang, P.; Chen, H.-Y.; Huang, S. Single Molecule Ratcheting Motion of Peptides in a Mycobacterium

Smegmatis Porin A (MspA) Nanopore. *Nano Lett.* **2021**, *21* (15), 6703−6710.
(16) Craig, J. M.; Laszlo, A. H.; Brinkerhoff, H.; Derrington, I. M.; Noakes, M. T.; Nova, I. C.; Tickman, B. I.; Doering, K.; de Leeuw, N. F.; Gundlach, J. H. Revealing Dynamics of Helicase Translocation on Single-Stranded DNA Using High-Resolution Nanopore Tweezers. *Proc. Natl. Acad. Sci. U. S. A.* **2017**, *114* (45), 11932−11937.
(17) Nova, I. C.; Ritmejeris, J.; Brinkerhoff, H.; Koenig, T. J. R.; Gundlach, J. H.; Dekker, C. Detection of Phosphorylation Post-Translational Modifications along Single Peptides with Nanopores. *Nat. Biotechnol.* **2024**, *42* (5), 710−714.
(18) Chen, X.; van de Sande, J. W.; Ritmejeris, J.; Wen, C.; Brinkerhoff, H.; Laszlo, A. H.; Albada, B.; Dekker, C. Resolving Sulfation Posttranslational Modifications on a Peptide Hormone Using Nanopores. *ACS Nano* **2024**, *18* (42), 28999−29007.
(19) Ke, W.; Wu, P.; Ma, S.; Yang, Y.; Zhang, Y.; Zhang, Q.; Lu, X.; Xia, B.; Wen, L.; Bai, J.; Gao, Z. Motor Protein-Assisted Glycan Translocation and Sequencing Using Nanopores. *bioRxiv* **2024**.
(20) De Rosa, L.; Di Stasi, R.; Romanelli, A.; D'Andrea, L. D. Exploiting Protein N-Terminus for Site-Specific Bioconjugation. *Molecules* **2021**, *26* (12), 3521.
(21) Dawson, P. E.; Muir, T. W.; Clark-Lewis, I.; Kent, S. B. H. Synthesis of Proteins by Native Chemical Ligation. *Science* **1994**, *266* (5186), 776−779.
(22) Thapa, P.; Zhang, R.-Y.; Menon, V.; Bingham, J.-P. Native Chemical Ligation: A Boon to Peptide Chemistry. *Molecules* **2014**, *19* (9), 14461−14483.
(23) Scheck, R. A.; Dedeo, M. T.; Iavarone, A. T.; Francis, M. B. Optimization of a Biomimetic Transamination Reaction. *J. Am. Chem. Soc.* **2008**, *130* (35), 11762−11770.
(24) Dempsey, D. R.; Jiang, H.; Kalin, J. H.; Chen, Z.; Cole, P. A. Site-Specific Protein Labeling with N-Hydroxysuccinimide-Esters and the Analysis of Ubiquitin Ligase Mechanisms. *J. Am. Chem. Soc.* **2018**, *140* (30), 9374−9378.
(25) MacDonald, J. I.; Munch, H. K.; Moore, T.; Francis, M. B. One-Step Site-Specific Modification of Native Proteins with 2-Pyridinecarboxyaldehydes. *Nat. Chem. Biol.* **2015**, *11* (5), 326−331.
(26) Filius, M.; van Wee, R.; de Lannoy, C.; Westerlaken, I.; Li, Z.; Kim, S. H.; de Agrela Pinto, C.; Wu, Y.; Boons, G.-J.; Pabst, M.; de Ridder, D.; Joo, C. Full-Length Single-Molecule Protein Fingerprinting. *Nat. Nanotechnol.* **2024**, *19*, 652−659.
(27) Bridge, H. N.; Leiter, W.; Frazier, C. L.; Weeks, A. M. An N Terminomics Toolbox Combining 2-Pyridinecarboxaldehyde Probes and Click Chemistry for Profiling Protease Specificity. *Cell Chem. Biol.* **2024**, *31* (3), 534−549.e8.
(28) Barber, L. J.; Stankevich, K. S.; Spicer, C. D. Effect of Pyridinecarboxaldehyde Functionalization on Reactivity and N-Terminal Protein Modification. *JACS Au* **2025**, *5* (4), 1983−1991.
(29) Guimaraes, C. P.; Witte, M. D.; Theile, C. S.; Bozkurt, G.; Kundrat, L.; Blom, A. E. M.; Ploegh, H. L. Site-Specific C-Terminal Internal Loop Labeling of Proteins Using Sortase-Mediated Reactions. *Nat. Protoc.* **2013**, *8* (9), 1787−1799.
(30) Antos, J. M.; Truttmann, M. C.; Ploegh, H. L. Recent Advances in Sortase-Catalyzed Ligation Methodology. *Curr. Opin. Struct. Biol.* **2016**, *38*, 111−118.
(31) Niemeyer, C. M. Semisynthetic DNA−Protein Conjugates for Biosensing and Nanofabrication. *Angew. Chem., Int. Ed.* **2010**, *49* (7), 1200−1216.
(32) Williams, B. A. R.; Chaput, J. C. Synthesis of Peptide-Oligonucleotide Conjugates Using a Heterobifunctional Crosslinker. *Curr. Protoc. Nucleic Acid Chem.* **2010**, *42* (1), 4.41.1−4.41.20.
(33) Schmidt, M.; Toplak, A.; Quaedflieg, P. J. L. M.; Ippel, H.; Richelle, G. J. J.; Hackeng, T. M.; van Maarseveen, J. H.; Nuijens, T. Omniligase-1: A Powerful Tool for Peptide Head-to-Tail Cyclization. *Adv. Synth. Catal.* **2017**, *359* (12), 2050−2055.
(34) Toplak, A.; Teixeira de Oliveira, E. F.; Schmidt, M.; Rozeboom, H. J.; Wijma, H. J.; Meekels, L. K. M.; de Visser, R.; Janssen, D. B.; Nuijens, T. From Thiol-Subtilisin to Omniligase: Design and Structure of a Broadly Applicable Peptide Ligase. *Comput. Struct. Biotechnol. J.* **2021**, *19*, 1277−1287.
(35) Bloom, S.; Liu, C.; Kölmel, D. K.; Qiao, J. X.; Zhang, Y.; Poss, M. A.; Ewing, W. R.; MacMillan, D. W. C. Decarboxylative Alkylation for Site-Selective Bioconjugation of Native Proteins via Oxidation Potentials. *Nat. Chem.* **2018**, *10* (2), 205−211.
(36) Zhang, L.; Floyd, B. M.; Chilamari, M.; Mapes, J.; Swaminathan, J.; Bloom, S.; Marcotte, E. M.; Anslyn, E. V. Photoredox-Catalyzed Decarboxylative C-Terminal Differentiation for Bulk- and Single-Molecule Proteomics. *ACS Chem. Biol.* **2021**, *16* (11), 2595−2603.
(37) Hong, V.; Steinmetz, N. F.; Manchester, M.; Finn, M. G. Labeling Live Cells by Copper-Catalyzed Alkyne−Azide Click Chemistry. *Bioconjugate Chem.* **2010**, *21* (10), 1912−1916.
(38) Zapadka, K. L.; Becher, F. J.; Gomes dos Santos, A. L.; Jackson, S. E. Factors Affecting the Physical Stability (Aggregation) of Peptide Therapeutics. *Interface Focus* **2017**, *7* (6), 20170030.
(39) Li, R.; Schmidt, M.; Zhu, T.; Yang, X.; Feng, J.; Tian, Y.; Cui, Y.; Nuijens, T.; Wu, B. Traceless Enzymatic Protein Synthesis without Ligation Sites Constraint. *Natl. Sci. Rev.* **2022**, *9* (5), No. nwab158.
(40) Gimeno, A.; Ehlers, A. M.; Delgado, S.; Langenbach, J.-W. H.; van den Bos, L. J.; Kruijtzer, J. A. W.; Guigas, B. G. A.; Boons, G.-J. Site-Specific Glyco-Tagging of Native Proteins for the Development of Biologicals. *J. Am. Chem. Soc.* **2024**, *146* (50), 34452−34465.
(41) Lu, C.; Bonini, A.; Viel, J. H.; Maglia, G. Toward Single-Molecule Protein Sequencing Using Nanopores. *Nat. Biotechnol.* **2025**, *43* (3), 312−322.
(42) Sauciuc, A.; Whittaker, J.; Tadema, M.; Tych, K.; Guskov, A.; Maglia, G. Blobs Form during the Single-File Transport of Proteins across Nanopores. *Proc. Natl. Acad. Sci. U. S. A.* **2024**, *121* (38), No. e2405018121.
(43) Chen, Z.; Wang, J.; Meng, X.; Ye, F.; Wang, L.; Xu, Y.; Wang, X.; Wang, Q.; Wen, H.; Bai, J. Spike Signals and MD Simulations Reveal the Significance of Peptide Stretching in Nanopore Protein Sequencing. *J. Am. Chem. Soc.* **2025**, *147*, 24347.
(44) Petitjean, F.; Ketterlin, A.; Gançarski, P. A Global Averaging Method for Dynamic Time Warping, with Applications to Clustering. *Pattern Recognit.* **2011**, *44* (3), 678−693.
(45) Asandei, A.; Schiopu, I.; Chinappi, M.; Seo, C. H.; Park, Y.; Luchian, T. Electroosmotic Trap Against the Electrophoretic Force Near a Protein Nanopore Reveals Peptide Dynamics During Capture and Translocation. *ACS Appl. Mater. Interfaces* **2016**, *8* (20), 13166−13179.
(46) Huang, G.; Willems, K.; Soskine, M.; Wloka, C.; Maglia, G. Electro-Osmotic Capture and Ionic Discrimination of Peptide and Protein Biomarkers with FraC Nanopores. *Nat. Commun.* **2017**, *8* (1), 935.
(47) Restrepo-Pérez, L.; Wong, C. H.; Maglia, G.; Dekker, C.; Joo, C. Label-Free Detection of Post-Translational Modifications with a Nanopore. *Nano Lett.* **2019**, *19* (11), 7957−7964.
(48) Yu, L.; Kang, X.; Li, F.; Mehrafrooz, B.; Makhamreh, A.; Fallahi, A.; Foster, J. C.; Aksimentiev, A.; Chen, M.; Wanunu, M. Unidirectional Single-File Transport of Full-Length Proteins through a Nanopore. *Nat. Biotechnol.* **2023**, *41* (8), 1130−1139.
(49) Sauciuc, A.; Morozzo della Rocca, B.; Tadema, M. J.; Chinappi, M.; Maglia, G. Translocation of Linearized Full-Length Proteins through an Engineered Nanopore under Opposing Electrophoretic Force. *Nat. Biotechnol.* **2024**, *42*, 1275−1281.
(50) Martin-Baniandres, P.; Lan, W. H.; Board, S.; Romero-Ruiz, M.; Garcia-Manyes, S.; Qing, Y.; Bayley, H. Enzyme-Less Nanopore Detection of Post-Translational Modifications within Long Polypeptides. *Nat. Nanotechnol.* **2023**, *18*, 1335.

https://doi.org/10.1021/jacs.5c18813
J. Am. Chem. Soc. 2026, 148, 3433−3441